EURASIP Journal on Wireless Communications and Networking 2005:5, 816–827


# Optimum Antenna Downtilt Angles for Macrocellular WCDMA Network

**Jarno Niemelä**
*Institute of Communications Engineering, Tampere University of Technology, P.O. BOX 553, 33101 Tampere, Finland*
*Email: jarno.niemela@tut.fi*

**Tero Isotalo**
*Institute of Communications Engineering, Tampere University of Technology, P.O. BOX 553, 33101 Tampere, Finland*
*Email: tero.isotalo@tut.fi*

**Jukka Lempiäinen**
*Institute of Communications Engineering, Tampere University of Technology, P.O. BOX 553, 33101 Tampere, Finland*
*Email: jukka.lempiainen@tut.fi*

*Received 3 January 2005; Revised 12 May 2005; Recommended for Publication by Pascal Chevalier*

The impact of antenna downtilt on the performance of cellular WCDMA network has been studied by using a radio network planning tool. An optimum downtilt angle has been evaluated for numerous practical macrocellular site and antenna configurations for electrical and mechanical antenna downtilt concepts. The aim of this massive simulation campaign was expected to provide an answer to two questions: firstly, how to select the downtilt angle of a macrocellular base station antenna? Secondly, what is the impact of antenna downtilt on system capacity and network coverage? Optimum downtilt angles were observed to vary between 3.5°–10.5° depending on the network configuration. Moreover, the corresponding downlink capacity gains varied between 0–58%. Antenna vertical beamwidth affects clearly the required optimum downtilt angle the most. On the other hand, with wider antenna vertical beamwidth, the impact of downtilt on system performance is not such imposing. In addition, antenna height together with the size of the dominance area affect the required downtilt angle. Finally, the simulation results revealed how the importance of the antenna downtilt becomes more significant in dense networks, where the capacity requirements are typically also higher.

**Keywords and phrases:** electrical downtilt, other-cell interference, mechanical downtilt, network coverage, system capacity, WCDMA.

## 1. INTRODUCTION

The majority of the current third-generation mobile communication systems use CDMA (code-division multiple access) technique as a multiple-access method. Due to its interference-limited nature, the system capacity of any cellular CDMA network is vulnerable to any additional other-cell interference. Therefore, in a CDMA radio network planning process, the main target is to plan the network in such a manner that other-cell interference is minimized in order to be able to maximize the system capacity. This can be achieved, among all other techniques, by optimizing the network topology. One important phase of the *topology planning*[1] is the definition of antenna configuration, and especially, antenna downtilt angle. By utilizing antenna downtilt, signal level within a cell can be improved and interference radiation towards other cells effectively reduced due to more precise aiming of the antenna radiation pattern. However, an excessive downtilt angle might lead to coverage problems at cell border areas. Therefore, it is vital to define an optimum downtilt angle separately for each site and antenna configuration.

Antenna downtilt includes two different concepts—mechanical downtilt (MDT) and electrical downtilt (EDT).



[1] The target of topology planning is to optimize site and antenna configuration in such a manner that cells become as isolated as possible.

Utilization of antenna mechanical downtilt has been a tool for radio network planners to optimize networks. It has been observed to be an efficient method to reduce other-cell interference in the main-lobe direction [1]. Hence, MDT is widely used in TDMA/FDMA (time-division multiple access/frequency-division multiple access) networks as in GSM (Global System for Mobile Communications) to decrease co-channel interference. However, in GSM, utilization of downtilt targets in achieving a smaller frequency reuse factor. Therefore, any improvements in the radio network quality due to antenna downtilt have not been directly taken into account in capacity or frequency planning phases in practice, but have been used as an extra margin to avoid serious interference areas [2]. Nevertheless, capacity gains up to 20% have been reported from utilization of MDT in GSM networks [3]. This reduction of other-cell interference affects especially macrocellular WCDMA (wideband CDMA) networks [4], where the achievable capacity gain from MDT has been observed to vary between 15% and 20% [5, 6, 7]. Moreover, MDT is able to enhance system capacity in microcellular environment [8, 9], even though the contribution of other-cell interference is typically smaller in microcellular environment.

In an interference-limited WCDMA system, suppression of side and back lobes of an antenna would be advantageous due to further reduction of other-cell interference. Therefore, electrically downtilted antennas might become an attractive choice for antenna selection. In EDT, the vertical radiation pattern is uniformly downtilted in all horizontal directions—contrary to mechanical downtilt. Prior work [10] have reported capacity gains up to 50% and 20% for 3-sectored and 6-sectored sites, respectively, with corresponding optimum downtilt angles of 7°–10°. On the contrary, in [11], optimum EDT angles have been defined on site-by-site basis using an iterative algorithm. Moreover, optimum downtilt angles were found to vary between 6°–8°, and to provide capacity gain up to 15% with practical macrocellular network configurations. Naturally, an increasing impact of EDT on the system capacity has been observed in microcellular environment as well [12]. Recently, one direction of research concerning antenna downtilt has been concentrated on adaptively and remotely controlled EDT according to changes in the load or user distribution within a cell [13]. Compared to utilization of a static network-wide downtilt angle, dynamically changing downtilt angle can further boost the system capacity by 20–30% under certain circumstances [14].

The aim of this paper is to extend the prior work of the authors in [7, 15], to present a simultaneous analysis of mechanical and electrical antenna downtilt concepts in WCDMA macrocellular network, and to evaluate optimum downtilt angles for different practical base station site and antenna configurations for suburban environment by utilizing a static radio network planning tool. Furthermore, the target is to identify and analyze the most important phenomena resulting from utilization of antenna downtilt and to clarify the sensitivity of the selection of downtilt angle. Finally, capacity gains of network-wide static antenna downtilt are provided for all simulated network configurations.

## 2. CAPACITY OF WCDMA NETWORK

In cellular WCDMA system, the same carrier frequency is used in all cells, and users are separated by unique code sequences. The capacity of WCDMA system is thus typically interference-limited rather than blocking-limited, since all mobiles and base stations interfere with each others in uplink and downlink directions. Furthermore, the network (or cell) capacity is defined by the load equations that, on the other hand, set limits for the maximum number of users in a cell or for the maximum cell throughput. The system capacity is defined in this context as the maximum number of users that can be supported simultaneously with a predefined service probability target.

### 2.1. Uplink capacity

Energy-per-bit-to-noise spectral density ratio, $E_b/N_0$, is used to measure the quality of a connection. In the uplink (UL) direction, the signal quality received at the base station for the $j$th user must satisfy the following condition:

$$\left(\frac{E_b}{N_0}\right)_j = \frac{(W/R_j)\,p_{\mathrm{TX},j}}{P_{\mathrm{RX}}^{\mathrm{BS}} L_j - p_{\mathrm{TX},j}}, \tag{1}$$

where $W$ is the system chip rate, $R_j$ is the bit rate of the $j$th mobile, $p_{\mathrm{TX},j}$ is the transmit (TX) power of the $j$th mobile, $P_{\mathrm{RX}}^{\mathrm{BS}}$ is the total received wideband power[2] at the base station, and $L_j$ is the uplink path loss from the $j$th mobile to the base station. The maximum uplink capacity is defined by the uplink load factor, $\eta_{\mathrm{UL}}$, which is given as interference rise above the thermal noise power:

$$\eta_{\mathrm{UL}} = \frac{P_{\mathrm{RX}}^{\mathrm{BS}} - p_n}{P_{\mathrm{RX}}^{\mathrm{BS}}}, \tag{2}$$

where $p_n$ is the thermal noise power at the base station.

The load factor is used to define a radio network planning parameter called interference margin[3] (IM) that takes into account the changes in the network coverage due to cell breathing:

$$\mathrm{IM} = -10\log_{10}(1-\eta_{\mathrm{UL}}). \tag{3}$$

### 2.2. Downlink capacity

The capacity of the downlink (DL) in WCDMA system behaves differently compared to the uplink. This is caused by the fact that all mobiles share the same transmit power of a base station sector. Furthermore, simultaneous transmission allows the usage of orthogonal codes. However, the code orthogonality $\alpha$ is partly destroyed by multipath propagation, which depends on the propagation environment, mobile speed, and mobile location. In order to satisfy the $E_b/N_0$

[2] The total wideband power includes thermal noise, and received powers from mobiles in own cell as well as from other cells.

[3] Interference margin is also called noise rise.

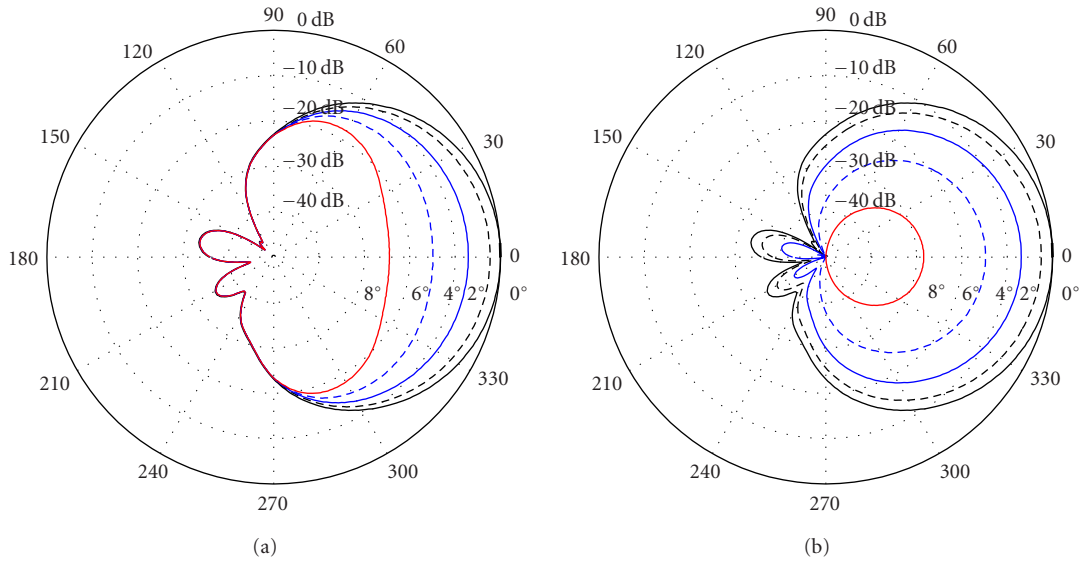


Figure 1: The impact of antenna (a) mechanical and (b) electrical downtilts on the horizontal (azimuthal) radiation pattern in the boresight. Antenna gain is normalized to zero and the scale is in decibels. "Uptilt" of back-lobe direction for mechanical downtilt is not illustrated.

requirement of the $k$th mobile in the DL, the following criterion has to be fulfilled:

$$\left(\frac{E_b}{N_0}\right)_k = \frac{(W/R_k)p_{\mathrm{TCH},k}}{P_{\mathrm{RX}}^{\mathrm{MS}}L_k - \alpha P_{\mathrm{TX}}^{\mathrm{TOT}} - (1-\alpha)p_{\mathrm{TCH},k}}. \quad (4)$$

In (4), $p_{\mathrm{TCH},k}$ is the downlink traffic channel (TCH) TX power for the $k$th connection, $P_{\mathrm{RX}}^{\mathrm{MS}}$ is the total received wideband power at the mobile station, $L_k$ is the downlink path loss, and $P_{\mathrm{TX}}^{\mathrm{TOT}}$ is the total TX power of a base station the sector mobile is connected to. The parameter $P_{\mathrm{TX}}^{\mathrm{TOT}}$ includes the TX power of common pilot channel (CPICH), other common channels (CCCH), and traffic channels as well. The total transmit power $P_{\mathrm{TCH},m}^{\mathrm{TOT}}$ for the TCH of the $m$th base station sector is thus the sum of all $K$ connections (including soft and softer handover connections):

$$P_{\mathrm{TCH},m}^{\mathrm{TOT}} = \sum_{k=1}^{K} p_{\mathrm{TCH},k}. \quad (5)$$

The downlink load factor, $\eta_{\mathrm{DL}}$, is defined with the aid of the average transmit power of TCHs of base stations for a cluster of cells:

$$\eta_{\mathrm{DL}} = \frac{\sum_{m=1}^{M} P_{\mathrm{TCH},m}^{\mathrm{TOT}}}{MP_{\mathrm{TCH},m}^{\max}}, \quad (6)$$

where $M$ is the number of sectors in the cluster. The downlink capacity is maximized when the minimum $\eta_{\mathrm{DL}}$ is achieved with the same number of served users $K$.

## 3. ANTENNA DOWNTILT

### 3.1. Downtilt concepts

In mechanical downtilt (MDT), the antenna element is physically directed towards the ground. Naturally, the areas near the base station experience better signal level due to the fact that the antenna main lobe is more precisely directed towards the intended dominance (serving) area. However, the effective downtilt angle corresponds to the physical one only exactly in the main-lobe direction, and decreases as a function of horizontal direction in such a way that the antenna radiation pattern is not downtilted at all in the side-lobe direction [1]. Nevertheless, interference radiation towards other cells is reduced in the main-lobe direction. The relative widening of the horizontal radiation pattern is illustrated in Figure 1a for a horizontally 65° and vertically 6° wide antenna beam as a function of increasing downtilt angle. The reduction of the antenna gain towards the boresight, for example, with 8° downtilt angle, is as large as 25 dB, whereas towards 60° angle the reduction is less than 10 dB.

As the downtilt angle increases, the soft handover (SHO) probability in the cell border areas decreases [16]. On the other hand, the relative widening of the horizontal radiation pattern increases the overlapping between adjacent sectors, which makes softer handovers (SfHO) more attractive. This increase of softer handovers as a function of downtilt angle depends on sector overlapping (i.e., sectoring and antenna horizontal beamwidth) [7, 17].

Antenna electrical downtilt (EDT) is carried out by adjusting the relative phases of antenna elements of an antenna array in such a way that the radiation pattern can be downtilted uniformly in all horizontal directions [18]. This technique changes slightly the vertical radiation pattern

depending on the chosen EDT angle. Figure 1b illustrates the behavior of the horizontal radiation pattern for 65° and vertically 6° wide antenna beam. EDT reduces efficiently radiation also towards the adjacent sectors, since all directions are downtilted uniformly. However, the coverage in the sidelobe direction reduces rapidly as well, which deteriorates the network performance if antennas are downtilted excessively. Naturally, SHO probability decreases as the downtilt angle increases, whereas SfHO probability should not change remarkably [15, 17].

### 3.2. Downtilt schemes

Fundamentally, there are two concepts for downtilt—mechanical and electrical. However, there exist many different tilting schemes including purely mechanical tilt, fixed electrical tilt, variable electrical tilt (VET), remote electrical tilt (RET), and continuously adjustable electrical downtilt (CAEDT). Adjusting antenna mechanical downtilt angle requires a site visit, which makes the adjustment process of tilt angles more expensive and time consuming. Hence, if MDT is utilized, the importance of the selection of an optimum mechanical tilt angle in the network deployment phase should be of great importance. Fixed electrical tilt antennas require also a site visit in order to change the tilt angle. However, if the fixed electrical tilt angle is wanted to change electrically, it requires a totally new antenna, or tilt angle is further increased/decreased purely mechanically (combined tilt scheme). In VET antennas, an electrical downtilt angle is adjustable in the dynamic range of downtilt angle. A typical range for tilt angles for macrocellular antennas vary from 0° to 12° depending on the vertical beamwidth [19, 20]. Utilization of RET scheme removes the need for a site visit, since tilt angles can be changed from network management system. Hence, it saves the costs and time in optimization during network evolution. An improvement of RET scheme is CAEDT scheme, in which downtilt angle can be changed continuously and remotely according to changes, for example, in propagation environment or in load distribution of a cell. Nevertheless, no matter what the utilized downtilt scheme is, knowledge about the initial optimum downtilt angle is needed in order to maximize the capacity and quality.

### 3.3. Selection of downtilt angle

The selection of antenna downtilt angle depends on the site and antenna configuration, and hence it has to be set on site-by-site basis in practice. In WCDMA, an optimum downtilt angle is obviously a tradeoff between other-cell interference mitigation and coverage thresholds. The optimum downtilt angle is achieved if other-cell interference is reduced to the minimum achievable level while still providing the target coverage.

An optimum downtilt angle—either for MDT or EDT—depends partly on the same factors. Perhaps two most obvious ones are the geometrical factor ($\theta_{\text{geo}}$) and antenna vertical beamwidth factor ($\theta_{\text{ver}}^{\text{BW}}$). The geometrical factor takes into account the average height difference between the base station ($h_{\text{BS}}$) and mobile station antenna ($h_{\text{MS}}$) as well as the size of the sector dominance area ($d$):

$$\theta_{\text{geo}} = \arctan\left(\frac{h_{\text{BS}} - h_{\text{MS}}}{d}\right). \tag{7}$$

Intuitively, an increase of the antenna height should also increase the required downtilt angle and vice versa. Correspondingly, a cell with a small dominance area should require a larger downtilt angle. However, the geometrical factor as such is not enough to define the required downtilt angle, as it does not take into account any information about antenna vertical beamwidth. One possibility is to select the antenna beamwidth factor as half of the antenna half-power (−3 dB) vertical beamwidth ($\theta_{-3\,\text{dB}}$). Thus, the selection of geometrical downtilt angle ($\nu_{\text{geo}}$) could be performed as in [21]:

$$\nu_{\text{geo}} = \theta_{\text{geo}} + \frac{\theta_{-3\,\text{dB}}}{2}. \tag{8}$$

## 4. SIMULATIONS

### 4.1. Network configuration

The impact of different network configurations on the optimum downtilt angles is simulated by using a static WCDMA radio network simulator that utilizes Monte Carlo technique for capacity and performance analysis. For the system-level analysis, a macrocellular network is configured in a shape of a regular hexagonal grid of 19 base stations. The selected antenna heights—25 m, 35 m, and 45 m—exceed the average roof-top level that dominates in the simulation area. The site spacings in the simulations are 1.5 km, 2.0 km, and 2.5 km. The sectoring schemes adopted in the simulation are 3-sectored and 6-sectored sites. Moreover, the base station antennas are oriented to have equal directions (see Figure 2). For the 3-sectored sites, the horizontal beamwidth (BW) of the antennas is 65° and vertical one either 6° or 12° with corresponding antenna gains of 18 dBi and 15.2 dBi. On the contrary, for the 6-sectored sites, horizontally 33° beamwidth and vertically 6° beamwidth antennas are utilized with corresponding antenna gain of 21 dBi. All radiation patterns of the base station antennas are adopted from [19]. Finally, the selected site and antenna configurations are the following:[4]

(i) EDT 3-sectored sites with 65°/6°,
(ii) EDT 3-sectored sites with 65°/12°,
(iii) EDT 6-sectored sites with 33°/6°,
(iv) MDT 3-sectored sites with 65°/6°,
(v) MDT 3-sectored sites with 65°/12°,
(vi) MDT 6-sectored sites with 33°/6°.

Morphological and topographic information of the simulation area is defined by a high resolution (5 m×5 m) digital map. The digital map includes the basic terrain types (water, open, and forest) and buildings of different heights in a

[4] 65°/6° denotes horizontal/vertical half-power beamwidth.

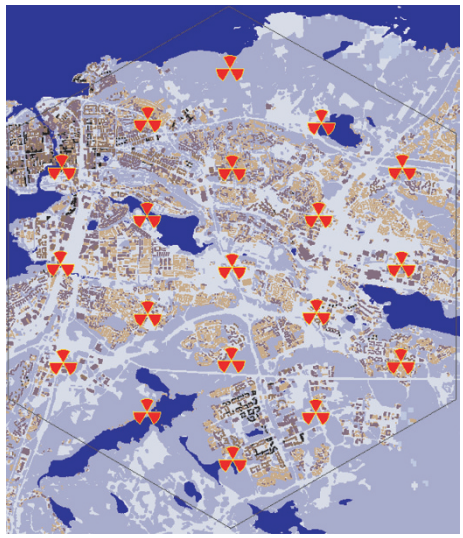

Figure 2: A 3-sectored hexagonal grid of 19 base stations with 2.0 km site spacing over the digital map. A 6-sectored configuration is formed based on 3-sectored antenna directions by adding antennas between the 3-sectored antennas. Traffic is distributed only inside the large hexagon.

Table 1: Morphological correction factors for extended COST-231-Hata model for different clutter types.

| Morphotype | Correction factor (dB) |
|---|---|
| Open | −17 |
| Water | −24 |
| Forest | −10 |
| Building height < 8 m | −4 |
| Building height > 8 m | −3 |
| Building height > 15 m | 0 |
| Building height > 23 m | 3 |

raster format. The simulation area is a suburban area consisting mainly of low-height residential buildings, but also including some higher commercial buildings. The simulation area of 2.0 km site spacing with 3-sectored sites is depicted in Figure 2.

### 4.2. Simulation parameters

The simulations consist of coverage predictions and capacity analysis. First, a coverage map of the simulation area is created by using extended COST-231-Hata propagation model for each base station site configuration. The model is roughly tuned for the simulation area. The radio propagation slope of COST-231-Hata model is set to 35 dB/dec (25 m antenna height as reference) and the mobile station antennas to 1.5 m. The utilized area correction factor for different clutter types are shown in Table 1. Moreover, diffraction losses are modeled with Deygout model embedded in the propagation model.

In the capacity analysis during Monte Carlo process, a large number of randomized snapshots are taken in order to simulate service establishments in the network. The total number of mobiles in one snapshot follows Poisson distribution with a mean number of mobiles provided as an input for the simulator. Hence, the number of mobile stations vary from snap shot to another, but over large number of statistically independent snap shots, the mean value is achieved. At the beginning of each snapshot, base stations and mobile stations' powers are initialized to the level of thermal noise power. Thereafter, the path losses of coverage map are adjusted with mobile-dependent slow fading standard deviations. After this initialization, the transmit powers for each link between the base station and mobile station are calculated *iteratively* in such a manner that $E_b/N_0$ requirements for all connections are satisfied according to (1) and (4) for UL and DL, respectively. During a snapshot, a mobile performs a service connection establishment to a sector, which provides the best $E_c/N_0$ on the CPICH:

$$\left(\frac{E_c}{N_0}\right) = \frac{p_{\text{CPICH}}}{P_{\text{RX}} L_k}, \tag{9}$$

where $p_{\text{CPICH}}$ is the power of CPICH of the corresponding sector and $P_{\text{RX}}$ is the total received wideband power. A mobile is put to outage during a snapshot, if target $E_b/N_0$ is not reached in either UL or DL, or the required $E_c/N_0$ is not achieved in the DL. Also, the UL noise rise of a cell should not exceed the given 6 dB limit during connection establishments.[5] The ratio between successful connection attempts and attempted connections during all snapshots is defined as *service probability*. After a successful service establishment, all other sectors are examined to see whether they satisfy the requirement to be in the active set (AS) of the mobile. If multiple $E_c/N_0$'s from different sectors are within the soft handover (SHO) window, a SHO connection is established supposing that all criteria for a successful connection are achieved with all sectors in the AS. After each snapshot, statistics are gathered and a new snapshot is started. For every network configuration, at least 10 000 independent snapshots are taken. Presented results in the following section are averaged over all these snapshots.

General simulation parameters are gathered in Table 2. In most of the simulations, homogenous user distribution consisting of speech users is used. Afterwards, a part of the simulation scenarios is carried out by using a traffic mix of speech and data users with a nonuniform distribution. Table 3 introduces service type related parameters.

## 5. SIMULATION RESULTS

### 5.1. Optimum downtilt angles

Every site and antenna configuration is simulated with two different traffic volumes (referred to as low and high). The same downtilt angle is utilized for all antennas in the network (a network-wide downtilt angle). This approach targets in solving an expected average optimum downtilt angle

[5] Cell noise rise is defined in (3).

Table 2: General simulation parameters.

| Parameter | Value |
|---|---|
| BS TX $P_{max}$ (dBm) | 43 |
| Max. BS TX per connection (dBm) | 38 |
| BS noise figure (dB) | 5 |
| CPICH TX power (dBm) | 33 |
| CCCH TX power (dBm) | 33 |
| SHO window (dB) | 4 |
| Outdoor/indoor STD for shadow fading (dB) | 8/12 |
| Building penetration loss (dB) | 15 |
| UL target noise rise limit (dB) | 6 |
| DL code orthogonality | 0.6 |
| Maximum active set size | 3 |

for a certain site and antenna configuration. Note that the target is not to seek the same downtilt angle for a part of a network, but to find an optimum downtilt angle depending on the site and antenna configuration. The definition of an optimum downtilt angle (ODA) is based on maximum service probability of low and high traffic volume scenarios. Hence, with an optimum downtilt angle, network coverage is guaranteed, and simultaneously, other-cell interference is mitigated as efficiently as possible. More detailed description of the definition method of ODA can be found from [15]. In the simulations, all downtilt angles are gradually increased in steps of 2°.

Table 4 gathers all optimum downtilt angles for all simulated network configurations. For all network configurations, ODAs increase as a function of antenna height and decrease as a function of site spacing. Generally, it can be observed that a change of ODA from 1.5 km to 2.0 km site spacing is higher than from 2.0 km to 2.5 km, hence indicating that a small downtilt angle should be always used. Moreover, with 12° antennas, the required downtilt angles are expectedly higher than for 6° antennas.

For the 3-sectored configurations with 6° vertical beamwidth, the optimum downtilt angle varies between 4.3°–8.1° depending on the network configuration and downtilt scheme. According to (7) and (8), the corresponding downtilt angles would have been 0.8°–2.5° and 3.8°–5.5°. The simulation results indicate that an increase of the antenna height changes expectedly the optimum downtilt angle; 10 m increase in the antenna height corresponds roughly to 1° increase of the ODA. On the other hand, site spacing has comparatively smaller impact on ODAs, especially with larger site spacings. In the 3-sectored configurations with 12° vertical beamwidth, the evaluated optimum downtilt angles range between 3.5°–10° (Table 4). With definitions of (7) and (8), the downtilt angles would have been 0.8°–2.5° and 6.8°–8.5°, respectively. On average, the ODAs are intuitively higher for the 12° than for 6° beamwidth. However, the increase of ODAs is not as huge as one could expect. One reason for even lower ODAs for 12° beamwidth are the interference conditions that differ due to lower antenna gain and wider vertical spread of antenna pattern. Without any downtilt with 6° beamwidth, the signal power is more precisely directed towards the boresight, whereas antennas of 12° beamwidth provide better coverage also in the areas closer to the base station in nontilted scenarios. This results in lower other-cell interference levels, but on the contrary, prevents high capacity gains.

An example plot of service probabilities and DL loads is given in Figure 3 for the 3-sectored network configurations with 1.5 km site spacing and 25 m antenna height under high traffic volume scenario. Moreover, curves are provided for both downtilt concepts and vertical beamwidths. Without any downtilt, the service probability is lower due to high level of other-cell interference that results in higher DL load as well. Moreover, higher level of other-cell interference can be clearly seen as lower service probability for vertically narrower antennas. Towards the optimum angle, DL load decreases due to reduction of other-cell interference and SHO overhead. On the other hand, in MDT, the DL load increases after certain downtilt angle due to increasing overhead of SfHO connections, which obviously limits ODA as well. However, the differences in ODAs between EDT and MDT are slightly different with these two vertical beamwidths. The reason for smaller ODAs for EDT network with 6° beamwidth is the more efficient coverage reduction (see Section 5.3). However, with 12° beamwidth the coverage reduction is not that efficient due to the wider vertical beam, but ODA is limited by the increase of SfHO connections. These phenomena depend heavily on the shape and width of the horizontal radiation pattern, and hence, for example, for horizontally 90° or 120° wide antennas, the relation between ODA for EDT and MDT might have been somewhat different. For 6° vertical beamwidth, the variations in service probability and DL load as a function of downtilt angle are higher within the simulated range, which makes the selection of downtilt angle also more sensitive with narrower antenna beamwidths. Thus, the results clearly indicate that antenna downtilt is not such critical for the sites equipped with vertically wide antennas, or in other words, the network capacity is not that sensitive to changes in the downtilt angle. However, it is reasonable to assume that downtilt of antenna with wider beamwidth becomes more important if the size of the dominance area becomes smaller like, for example, in urban areas.

With 6° beamwidth, selection of downtilt angle between 2°–8° would change the service probability with this particular traffic volume at maximum by 3%. In EDT, the gain in service probability is limited by coverage, but the gain in downlink capacity is higher as indicated in Figure 3b. The sensitivity of the selection of downtilt angle increases generally as a function of higher antenna position and shorter site spacing, that is, the more coverage overlapping, the higher the sensitivity. For 12° beamwidth, the selection of downtilt angle between 2°–10° would provide almost the same performance from the service probability perspective, but again slightly more significant gain is observed in the downlink.

In Table 4 for the 6-sectored configurations (only antennas of 6° vertical beamwidth simulated), the observed ODAs (4°–7°) are very close to the values of the corresponding 3-sectored configurations. In this scenario, (7) and (8) would

Table 3: Traffic and mobile profile characteristics for speech, real-time (RT) circuit-switched, and non-real-time (NRT) packet-switched services.

| Parameter | Speech | RT | NRT |
|---|---|---|---|
| UL/DL bit rate (kbps) | 12.2/12.2 | 64 / 64 | 64/128 |
| UL/DL $E_b/N_0$ (dB) | 5/8 | 3/5 | 3/5 |
| Activity factor | 0.5 | 1 | – |
| MS max. TX power (dBm) | 21 | 24 | 24 |
| MS TX power dynamic range (dB) | | 70 | |
| Required $E_c/I_0$ on CPICH (dB) | | −17 | |

Table 4: Optimum downtilt angles for mechanically and electrically downtilted antennas for all simulated site and antenna configurations. Evaluation of an optimum downtilt angle is based on a simple algorithm that utilizes information of resulting service probabilities with two different traffic volumes.

| Site spacing | Antenna height | EDT 3-sec. 6° | EDT 3-sec. 12° | EDT 6-sec. 6° | MDT 3-sec. 6° | MDT 3-sec. 12° | MDT 6-sec. 6° |
|---|---|---|---|---|---|---|---|
| 1.5 km | 25 m | 5.1° | 7.3° | 5.4° | 5.7° | 5.9° | 4.9° |
| | 35 m | 6.1° | 9.1° | 6.3° | 7.3° | 8.1° | 5.9° |
| | 45 m | 7.1° | 10.3° | 7.1° | 8.1° | 9.1° | 7.0° |
| 2.0 km | 25 m | 4.3° | 5.6° | 3.8° | 5.1° | 4.3° | 3.8° |
| | 35 m | 5.8° | 7.9° | 5.1° | 6.7° | 7.5° | 4.8° |
| | 45 m | 6.3° | 9.3° | 6.1° | 6.9° | 8.2° | 5.9° |
| 2.5 km | 25 m | 4.5° | 5.2° | 4.6° | 5.1° | 3.4° | 3.7° |
| | 35 m | 5.4° | 7.6° | 5.3° | 6.1° | 4.4° | 4.5° |
| | 45 m | 5.9° | 8.3° | 5.7° | 6.9° | 6.9° | 5.8° |

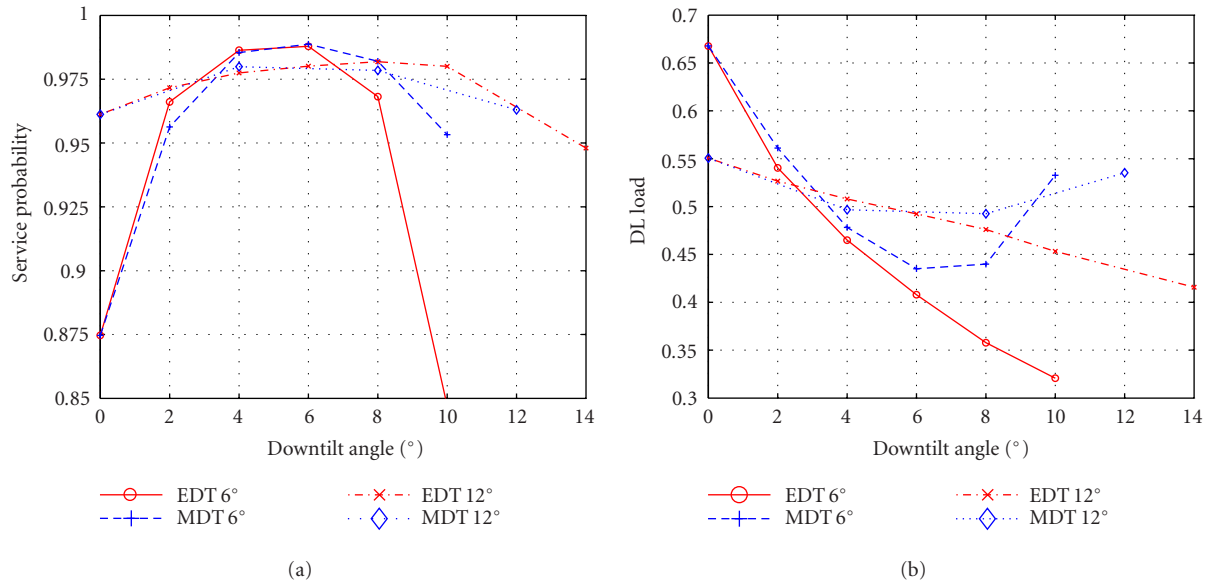


Figure 3: (a) Service probability and (b) DL load for the 3-sectored network configuration under high traffic volume. The network configuration consists of 1.5 km site spacing and 25 m antenna height together with either 6° or 12° vertical beamwidth.

have provided downtilt angles of 1.1°–3.3° and 4.1°–6.3°, respectively. Clearly, the latter values are relatively close to simulated ODA. With MDT, ODAs are at slightly lower level than with EDT. Moreover, they are also lower in the 6-sectored configuration than in the corresponding 3-sectored configuration. This can be explained with the fact that compared to 3-sectored sites, the relative sector overlapping is higher in 6-sectored site that makes the increase of SfHO a bigger issue. Looking at the example figure of the behavior of service probability in Figure 4a, it can be observed how selection of MDT angle is extremely sensitive. In this scenario, downtilt angle of 6° results in 30% better service probability and

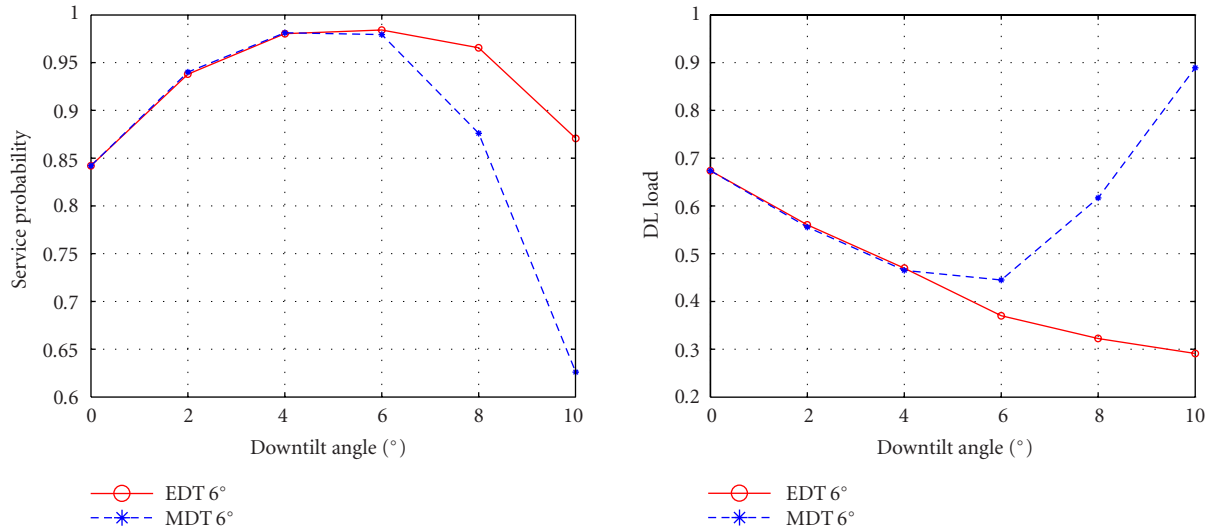


Figure 4: (a) Service probability and (b) DL load for the 6-sectored network configuration with high traffic volume. The network configuration consists of 1.5 km site spacing and 25 m antenna height together with 6° beamwidth.

45% lower DL load compared to 10° downtilt. The increase of SfHO connections is strongly related to the shape of horizontal radiation pattern, and, for example, in [7] such huge increase was not observed due to utilization of an antenna with lower side-lobe level. For the 6-sectored EDT configuration, the selection of the downtilt angle has been observed to be slightly more sensitive with respect to site spacing and antenna height than for the corresponding 3-sectored configuration. This is caused by relatively larger coverage overlapping (higher interference levels in the 6-sectored configuration). According to the results, the selection of antenna downtilt angle in the 6-sectored sites can follow the selected angles of the 3-sectored.

### 5.2. An empirical equation for selection of downtilt angle

The geometrical factor in (7) and the geometrical angle in (8) underestimate typically the required downtilt angle, especially with smaller site spacings and higher antenna positions (i.e., with larger overlapping). Therefore, an empirical equation is derived based on the simulated optimum downtilt angles:

$$\nu_{\text{opt}} = 3[\ln(h_{\text{BS}}) - d^{0.8}]\log_{10}(\theta_{-3\,\text{dB}}). \quad (10)$$

Equation (10) relates the topological factors such as the base station antenna height ($h_{\text{BS}}$ in meters), the intended length of the sector dominance area ($d$ in kilometers), and the half-power vertical beamwidth ($\theta_{-3\,\text{dB}}$ in degrees). The equation has been derived with a simple curve-fitting method. It provides a zero mean error with 0.5° standard deviation with respect to simulated optimum downtilt angles for all simulated scenarios. As the error of (10) is rather small, it could be embedded into a radio network planning tool. Thereafter, the tool would automatically provide a suggestion of downtilt angle for a planner based on the information of antenna vertical beamwidth, antenna height (also ground height level could be utilized), and expected dominance area of particular sector.

### 5.3. UL TX power and SfHO analysis

With high traffic volume (i.e., high network load), the factor that limits the service probability at low downtilt angles is the high level of other-cell interference. At higher downtilt angles, the service probability can be limited by several factors. In Figure 5a, an example of cumulative distribution function (CDF) of UL TX powers for the 6-sectored configuration is shown for nontilted scenario, and for 6° and 10° downtilt angles. For adequate downtilt angles (close to optimum), lower TX powers are allowed due to better bearing of antenna vertical pattern, especially close to the base station. On the other hand, the proportion of mobiles with high TX powers increases as well if high downtilt angles are utilized—particularly at the cell edges. With 10° EDT angle, UL TX powers are considerably higher than in the corresponding MDT network. This leads to a conclusion that UL TX power limits (i.e., UL $E_b/N_0$ target is not achieved) the ODAs in EDT network. Hence for EDT concept, at least one indicator of an excessive downtilt angle is a higher proportion of mobiles having high TX powers.

In MDT, the increase of DL load at higher downtilt angles is caused by the SfHO overhead. SfHO probability is given in Figure 5b as a function of downtilt angle for the 6° beamwidth in the 3-sectored and in the 6-sectored configurations with 25 m and 45 m antenna heights, and with 1.5 km site spacing. The increase of SfHO overhead is related to antenna horizontal beamwidth together with sectoring (sector overlapping) and to the shape of the horizontal

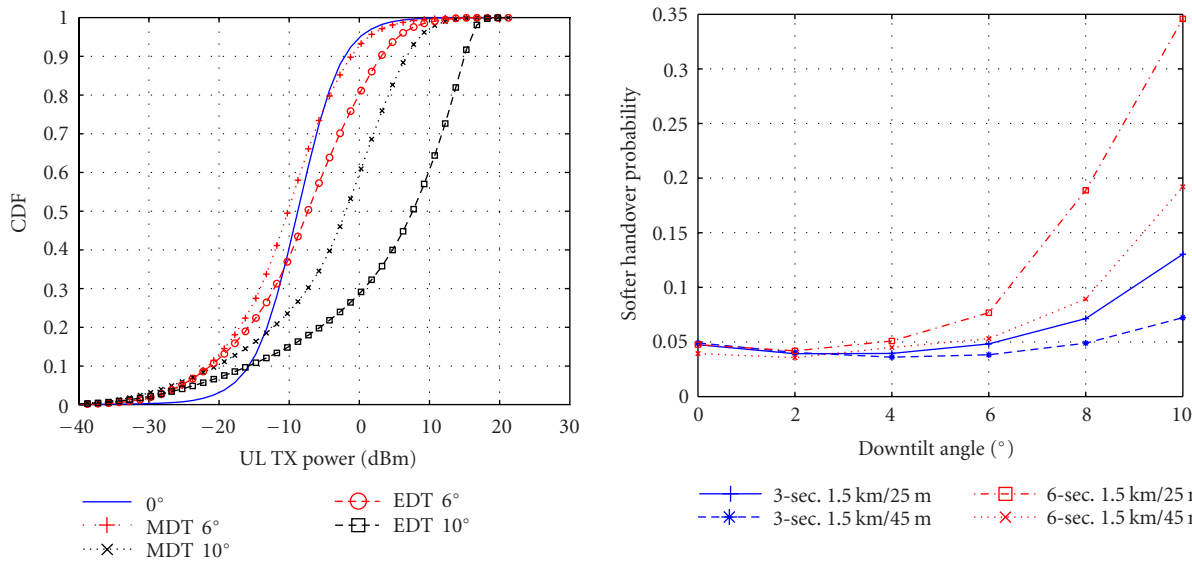


(a) (b)

Figure 5: (a) UL TX power distribution for the 6-sectored 1.5 km site spacing and 25 m antenna height configuration for nontilted, 6°, and 10° downtilt angles for MDT and EDT. Nontilted scenario is plotted with a solid line, MDT as dotted lines, and EDT as dashed lines. (b) Softer handover (SfHO) probability as a function of downtilt angle in MDT network for the 3-sectored configuration and the 6-sectored configuration in the topology of 1.5 km site spacing together with 25 m and 45 m antenna heights.

beam (e.g., side-lobe level). Moreover, Figure 5b indicates that this increase is more significant after 6° downtilt angle, which would also be a practical upper-limit for MDT angle, if SfHO overhead is wanted to be maintained at lower level. At the range of simulated downtilt angles, the SfHO probability is higher for smaller antenna heights due to geometrical reasons. However, the increase of SfHO overhead becomes more significant also with higher antenna position after downtilt angle of 10°. Hence, the increase of SfHO overhead clearly limits the service probability (rather than uplink coverage) and the range of optimum downtilt angles in MDT network.

### 5.4. Capacity gains

In Table 5, the capacity gains and corresponding maximum DL throughput of all configurations are shown. The capacity gains are evaluated between the closest optimum downtilt angle and the nontilted configuration. Moreover, the maximum DL throughput is based on 39 dBm average DL TX power (i.e., 0.5 DL load) of all sectors. According to the results in Table 5, the capacity gains vary from 0% up to 58% depending on the network configuration. Generally, the capacity gain becomes larger if the coverage overlapping increases, that is, either the antenna height increases or the site spacing decreases. Hence, considering an urban macrocellular environment, where the network is typically very dense due to requirements of higher coverage probabilities and capacity, utilization of antenna downtilt becomes more important.

The maximum DL throughput varies from 420 kbps to 525 kbps per sector. In most of the cases, EDT provides higher capacities with optimum downtilt angles than MDT. Moreover, the capacity gain is higher for the 6-sectored than for the 3-sectored network, which can be explained with higher initial coverage overlapping. Another observation is the increase of absolute sector capacity as a function of higher antenna position. Geometrically thinking, it is obvious that one can achieve higher capacity by increasing the antenna position due to better ability to aim the antenna beam towards the intended dominance area, and simultaneously decrease other-cell interference. However, a higher antenna position requires more precise adjustment of the antenna downtilt angle. Finally, it can be also concluded that antennas with narrower vertical beamwidth provide higher cell capacity.

### 5.5. Impact of traffic layer

In the preceding results, the traffic layer consisted only of homogenous distribution of speech users. As a verification simulation, a nonhomogenous traffic mix is used with the following user volumes and services:

(i) 50% of speech users (12.2 kbps);
(ii) 25% real-time circuit-switched data users (64 kbps);
(iii) 25% non-real-time packet-switched users (64/128 kbps).[6]

Detailed service parameters are given in Table 3. In the traffic mix, users are distributed such that 70% are indoors and 30% outdoors. An additional building penetration loss of 15 dB is allocated for indoor users. Moreover, the standard

[6]Packet service parameters were adopted from [22].

Table 5: Maximum sector throughput (kbps) for downlink with optimum downtilt angle and corresponding capacity gains with respect to nontilted scenario for all simulated network configurations. The maximum capacity values are based on 0.5 average DL load.

| Site spacing | Antenna height | EDT 3-sec 6° | EDT 3-sec 12° | EDT 6-sec 6° | MDT 3-sec 6° | MDT 3-sec 12° | MDT 6-sec 6° |
|---|---|---|---|---|---|---|---|
| 1.5 km | 25 m | 494 (18.1%) | 472 (2.8%) | 492 (27.5%) | 489 (17.0%) | 466 (1.6%) | 458 (18.8%) |
| | 35 m | 510 (33.5%) | 484 (12.1%) | 504 (43.8%) | 500 (30.8%) | 475 (9.9%) | 474 (35.3%) |
| | 45 m | 526 (48.4%) | 493 (18.7%) | 522 (58.1%) | 516 (45.6%) | 479 (15.4%) | 480 (45.5%) |
| 2.0 km | 25 m | 457 (8.0%) | 440 (1.4%) | 438 (9.4%) | 459 (8.5%) | 440 (1.4%) | 438 (9.3%) |
| | 35 m | 496 (17.8%) | 457 (4.3%) | 468 (22.5%) | 494 (17.4%) | 453 (3.3%) | 458 (20.0%) |
| | 45 m | 499 (27.7%) | 472 (8.0%) | 500 (37.5%) | 495 (26.8%) | 466 (6.6%) | 471 (29.4%) |
| 2.5 km | 25 m | 451 (5.3%) | 423 (0.8%) | 462 (6.3%) | 451 (5.3%) | 424 (1.1%) | 456 (5.0%) |
| | 35 m | 480 (9.9%) | 433 (2.1%) | 482 (16.9%) | 487 (11.5%) | 433 (2.0%) | 464 (12.5%) |
| | 45 m | 488 (20.4%) | 440 (2.6%) | 504 (31.3%) | 479 (18.3%) | 437 (2.0%) | 463 (20.6%) |

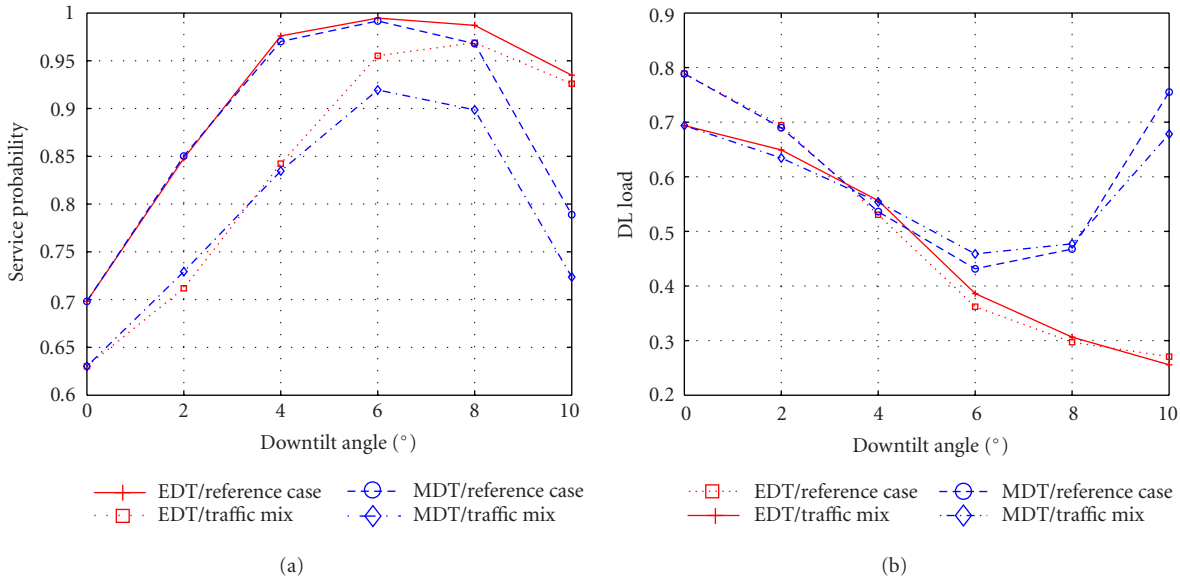


Figure 6: (a) Service probabilities and (b) DL load under traffic mix and nonhomogenous traffic distribution (70% indoors and 30% outdoors). Reference case curve shows the corresponding service probability from homogenous traffic simulations of speech users only.

deviation of slow fading is set to 12 dB in indoors. The network configuration of 6-sectored sites with 1.5 km site spacing and 35 m antenna height is taken as a reference for traffic mix simulations.

In the scenario of speech users only, the optimum downtilt angles are 5.9° and 6.3° for MDT and EDT, respectively (see Table 4). Figure 6a shows the average service probabilities under high user volume traffic mix and Figure 6b the corresponding DL loads. Under the traffic mix, the optimum downtilt angles for MDT are all slightly above 6°. For EDT, optimum downtilt angles would be roughly 7°. According to the results, the increase of SfHO connections obviously limits the ODA in MDT network independent of the traffic mix. On the contrary, the small shift in ODA of EDT network is caused by the higher maximum TX power capability (for data services 24 dBm). Hence, within the limits of downtilt angle setting in practice, the consistence of the traffic or its distribution does not affect the optimum downtilt angle.

## 6. DISCUSSION AND CONCLUSIONS

In the paper, the impact of antenna downtilt on the performance of cellular WCDMA network has been studied. An optimum downtilt angle, which is defined by the site spacing, antenna height, and vertical beamwidth, has been found for numerous practical network configurations. Within the range of typical macrocellular network configurations (site spacings of 1.5 km–2.5 km, antenna heights of 25 m–45 m, and antenna vertical beamwidths of 6°–12°), the optimum downtilt angle vary roughly between 3.5° and 10.5° for a

homogenous traffic distribution. The sectoring scheme (3-sectored or 6-sectored) and tilting concept (MDT or EDT) affect only in a smaller scale the selection of downtilt angle.

The behavior of EDT and MDT concepts from the WCDMA network performance point of view varies to some extent. In EDT, higher downtilt angles produce a greater proportion of mobile stations with high TX power that can easily lead to coverage problems. On the contrary in MDT, an excessive downtilt angle can cause an increase of SfHO overhead. However, this phenomenon depends heavily on the characteristics of the antenna horizontal radiation pattern and sectoring scheme. The increase of SfHO overhead is obviously one reason why the maximum DL sector capacities are smaller for MDT. However, the importance of antenna downtilt as a part of WCDMA topology optimization cannot be argued as the observed capacity gains from downtilting vary from 0% up to 58%. In general, capacity gain increases with higher antenna position and decreases with site spacing. Moreover, the narrower the antenna vertical beamwidth is, the higher the achievable capacity gain is. Also, the sensitivity of the selection of downtilt angle varies, mostly according to the antenna vertical beamwidth.

In certain circumstances, SHO can provide gain against the fast fading. Due to the fact that no gain was provided for a SHO connection, the observed capacity gain may be overestimated in the sense that in the nontilted scenarios, the SHO overhead was considerably higher than in the optimally downtilted scenario. This would also mean larger proportion of mobiles benefitting from the SHO gain. On the other hand, for example, in [23], antenna downtilt has been observed to decrease the delay spread, which would in turn lead to an increase of code orthogonality and to an improvement of the downlink capacity.

The traffic distribution between outdoors and indoors or traffic mix was not observed to have notable impact on the optimum downtilt angle. However, as the optimum downtilt angle was searched as an average of two different traffic volumes, it is heavily assumed that the optimum downtilt angle is more sensitive to changes in the amount of users and their location distribution within a cell. This proposes strongly to concentrate on algorithms for adaptive electrical downtilt schemes to further increase the capacity of WCDMA network.

## ACKNOWLEDGMENT

This work was supported by the European Communications Engineering (ECE) Ltd., Nokia Networks, FM Kartta, and National Technology Agency of Finland.

## REFERENCES

[1] D. J. Y. Lee and C. Xu, "Mechanical antenna downtilt and its impact on system design," in *Proc. IEEE 47th Vehicular Technology Conference (VTC '97)*, vol. 2, pp. 447–451, Phoenix, Ariz, USA, May 1997.

[2] J. Lempiäinen and M. Manninen, *Radio Interface System Planning for GSM/GPRS/UMTS*, Kluwer Academic, Dordrecht, The Netherlands, 2001.

[3] L. Zordan, N. Rutazihana, and N. Engelhart, "Capacity enhancement of cellular mobile network using a dynamic electrical down-tilting antenna system," in *Proc. IEEE VTS 50th Vehicular Technology Conference (VTC '99)*, vol. 3, pp. 1915–1918, Amsterdam, The Netherlands, September 1999.

[4] I. Forkel, A. Kemper, R. Pabst, and R. Hermans, "The effect of electrical and mechanical antenna down-tilting in UMTS networks," in *Proc. IEE 3rd International Conference on 3G Mobile Communication Technologies*, pp. 86–90, London, UK, May 2002.

[5] S. C. Bundy, "Antenna downtilt effects on CDMA cell-site capacity," in *Proc. IEEE Radio and Wireless Conference (RAWCON '99)*, pp. 99–102, Denver, Colo, USA, August 1999.

[6] M. J. Nawrocki and T. W. Wieckowski, "Optimal site and antenna location for UMTS output results of 3G network simulation software," in *Proc. 14th International Conference on Microwaves, Radar and Wireless Communications (MIKON '02)*, vol. 3, pp. 890–893, Gdansk, Poland, May 2002.

[7] J. Niemelä and J. Lempiäinen, "Impact of mechanical antenna downtilt on performance of WCDMA cellular network," in *Proc. IEEE 59th Vehicular Technology Conference (VTC '04)*, vol. 4, pp. 2091–2095, Milan, Italy, May 2004.

[8] H.-S. Cho, Y.-I. Kim, and D. K. Sung, "Protection against cochannel interference from neighboring cells using downtilting of antenna beams," in *Proc. IEEE VTS 53rd Vehicular Technology Conference (VTC '01)*, vol. 3, pp. 1553–1557, Rhodes, Greece, May 2001.

[9] J.-S. Wu, J.-K. Chung, and C.-C. Wen, "Hot-spot traffic relief with a tilted antenna in CDMA cellular networks," *IEEE Trans. Vehicular Technology*, vol. 47, no. 1, pp. 1–9, 1998.

[10] J. Laiho-Steffens, A. Wacker, and P. Aikio, "The impact of the radio network planning and site configuration on the WCDMA network capacity and quality of service," in *Proc. IEEE 51st Vehicular Technology Conference (VTC '00)*, vol. 2, pp. 1006–1010, Tokyo, Japan, May 2000.

[11] A. Wacker, K. Sipilä, and A. Kuurne, "Automated and remotely optimization of antenna subsystem based on radio network performance," in *Proc. 5th International Symposium on Wireless Personal Multimedia Communications (WPMC '02)*, vol. 2, pp. 752–756, Honolulu, Hawaii, USA, October 2002.

[12] D. H. Kim, D. D. Lee, H. J. Kim, and K. C. Whang, "Capacity analysis of macro/microcellular CDMA with power ratio control and tilted antenna," *IEEE Trans. Vehicular Technology*, vol. 49, no. 1, pp. 34–42, 2000.

[13] M. Garcia-Lozano and S. Ruiz, "Effects of downtilting on RRM parameters," in *Proc. 15th IEEE International Symposium on Personal, Indoor and Mobile Radio Communications (PIMRC '04)*, vol. 3, pp. 2166–2170, Barcelona, Spain, September 2004.

[14] M. Pettersen, L. E. Bråten, and A. G. Spilling, "Automatic antenna tilt control for capacity enhancement in UMTS FDD," in *Proc. IEEE 60th Vehicular Technology Conference (VTC '04)*, vol. 1, pp. 280–284, Los Angeles, Calif, USA, September 2004.

[15] T. Isotalo, J. Niemelä, and J. Lempiäinen, "Electrical antenna downtilt in UMTS network," in *Proc. 5th European Wireless Conference (EW '04)*, pp. 265–271, Barcelona, Spain, February 2004.

[16] J. Lempiäinen and M. Manninen, Eds., *UMTS Radio Network Planning, Optimization and QoS Management*, Kluwer Academic, Dordrecht, The Netherlands, 2003.

[17] J. Niemelä, "Impact of base station site and antenna configuration on capacity in WCDMA cellular networks," M.S. thesis, Tampere University of Technology, Tampere, Finland, 2003.

[18] G. Wilson, "Electrical downtilt through beam-steering versus mechanical downtilt [base station antennas]," in *Proc. IEEE*

*42nd Vehicular Technology Conference (VTC '92)*, vol. 1, pp. 1–4, Denver, Colo, USA, May 1992.
[19] Kathrein, *Technical information and new products*, 2004, available at: http://www.kathrein.de/.
[20] Radio Frequency Systems, RFS, 2004, available at: http://www.rfsworld.com/.
[21] J. Wu and D. Yuan, "Antenna downtilt performance in urban environments," in *Proc. IEEE Military Communications Conference (MILCOM '96)*, vol. 3, pp. 739–744, McLean, Va, USA, October 1996.
[22] ETSI, "Selection procedures for the choice of radio transmission technologies of the UMTS," TR 101 112, V3.2.0.
[23] E. Benner and A. B. Sesay, "Effects of antenna height, antenna gain, and pattern downtilting for cellular mobile radio," *IEEE Trans. Vehicular Technology*, vol. 45, no. 2, pp. 217–224, 1996.

**Jarno Niemelä** was born in Seinäjoki, Finland, in 1979. He received the M.S. degree in electrical engineering from Tampere University of Technology (TUT), Tampere, Finland, in 2003. Currently, he is working towards the Dr.Tech. degree as a researcher at Tampere University of Technology. His main research interests are topology planning of cellular WCDMA networks and mobile location techniques.

**Tero Isotalo** was born in Säkylä, Finland, in 1980. He is heading towards the M.S. degree in electrical engineering at Tampere University of Technology (TUT), Tampere, Finland. Currently, he is working at Tampere University of Technology, Institute of Communications Engineering. His main research interests are topology planning of cellular WCDMA networks for outdoor and indoor solutions.

**Jukka Lempiäinen** was born in Helsinki, Finland, in 1968. He received M.S., Lic.Tech., and Dr.Tech. degrees, all in electrical engineering, from Helsinki University of Technology, Espoo, Finland, in 1993, 1998, and 1999, respectively. He is a Senior Partner and CEO and President of the European Communications Engineering (ECE) Ltd. Before ECE Ltd., he worked more than five years in Nokia in different positions in the area of radio network planning and he has altogether more than 10 years experience in GSM-based mobile network planning and consulting. Currently, he is also a part-time Professor of telecommunications (radio network planning) at Tampere University of Technology, Tampere, Finland. He has written two international books about GSM/GPRS/UMTS cellular radio planning, several international journal and conference papers, and he has two patents. He has concentrated on the radio planning of the cellular networks during his whole career. His main interests are to combine the coverage- and capacity-related topics (topology planning in UMTS) and to adjust the performance of the technical details like diversity reception and GPRS traffic in the air interface. He is URSI National Board Member, Finland.